Evidence for Nodal Quasiparticles in the Nonmagnetic Superconductor YNi_2B_2C via Field-Angle-Dependent Heat Capacity

Tuson Park and M. B. Salamon
Department of Physics and Material Research Laboratory, University of Illinois at Urbana-Champaign, Illinois 61801

Eun Mi Choi, Heon Jung Kim, and Sung-Ik Lee
National Creative Research Initiative Center for Superconductivity and Department of Physics, Pohang University of Science and Technology, Pohang 790-784, Republic of Korea
(Received 7 October 2002; published 29 April 2003)

Field-angle dependent heat capacity of the nonmagnetic borocarbide superconductor YNi_2B_2C reveals a clear fourfold oscillation, the first observation of its kind. The observed angular variations were analyzed as a function of magnetic field angle, field-intensity, and temperature to provide its origin. The quantitative agreement between experiment and theory strongly suggests that we are directly observing nodal quasiparticles generated along $\langle 100 \rangle$ by the Doppler effect. The results demonstrate that field-angle heat capacity can be a powerful tool in probing the momentum-space gap structure in unconventional superconductors such as high T_c cuprates, heavy-fermion superconductors, etc.

DOI: 10.1103/PhysRevLett.90.177001 PACS numbers: 74.20.Rp, 74.25.Bt, 74.25.Jb, 74.70.Dd

Most superconductors behave "conventionally"; electronic excitations are suppressed by the BCS energy gap causing the electronic heat capacity, for example, to be exponentially small at temperatures well below the superconducting transition. Recently, a number of superconductors, cuprates and heavy-fermion metals among them, have been found to be "unconventional" in that they exhibit gap-zero (or nodal) points or lines in momentum space. Electronic excitations—nodal quasiparticles (nqp)—are then observed at low temperatures, giving rise to power-law rather than exponential behavior. Unlike gapless superconductivity, which can occur in conventional superconductors, the Fermi momenta of these quasiparticles are restricted to nodal regions of the Fermi surface, giving a strong directional dependence to various physical properties. While pioneering work by Yu *et al.* [1] and by subsequent experimenters [2,3] demonstrated the directionality of thermally excited nqp's via the thermal conductivity, direct detection has proven elusive [4].

The rare earth borocarbide superconductors RNi_2B_2C (R = Y, Lu, Tm, Er, Ho, and Dy) had been generally thought to exhibit isotropic s-wave pairing via electron-phonon coupling [5–9], but there is growing evidence that the gap function is highly anisotropic or has a nodal structure on the momentum surface [3,10–14]. In specific heat measurements, a power-law behavior was observed in the temperature dependence and the electronic coefficient $\gamma(H)$, to the extent it can be extracted, follows a square-root field dependence [10,15]. Low temperature thermal conductivity measurements also indicate unconventional superconductivity [11]. Recently, Izawa *et al.* reported a field-directional-angle dependence of the thermal conductivity in YNi_2B_2C that suggested point nodes along $\langle 100 \rangle$ directions [3]. However, their interpretation is not definitive because the highly anisotropic nature of the Fermi surface and nonlocality could lead to anisotropic macroscopic phenomena even within the ab plane [16]. We report here the first observation of Doppler-induced angular dependence of the electronic heat capacity in the nonmagnetic borocarbide superconductor YNi_2B_2C. Such measurements are, however, insensitive to Fermi-surface topology and reflect the gap anisotropy [17].

The inset of Fig. 1 shows the zero-field heat capacity of the single crystal YNi_2B_2C grown by the high temperature flux method using Ni_2B as a solvent [18]. ac calorimetry was used to measure the heat capacity [19]. The sharp thermodynamic transition ($\Delta T/T_c \leq 0.02$) indicates that the sample is homogeneous.

The main graph of Fig. 1 shows the field dependence of the heat capacity at 2.5 K. The sample was zero-field cooled to 2.5 K and a magnetic field was applied along the (100) direction. The open circles describe the heat capacity with increasing field, and the crosses with decreasing field. There is a deviation between the two below 1 T, which indicates that flux pinning is important at low magnetic fields. The system enters into the normal state above 5.2 T along this direction and the lower critical field is less than 0.1 T. The heat capacity with increasing magnetic field was fitted by $C_0 + b\,(H - H_0)^{1/2}$ (dashed line). The excellent square-root fit up to the upper critical field indicates that YNi_2B_2C is a superconductor with an unconventional pairing symmetry. In an intermediate field range, $H_{c1} \ll H \ll H_{c2}$, the square-root field dependence comes mostly from nqp's induced by the Doppler effect; the core-state contribution becomes important as the field approaches H_{c2} [15,20].

The upper panel of Fig. 2 shows the field-directional angular dependence of the total heat capacity at 2 K in 1 T. The field angle α was measured with respect to the a axis.

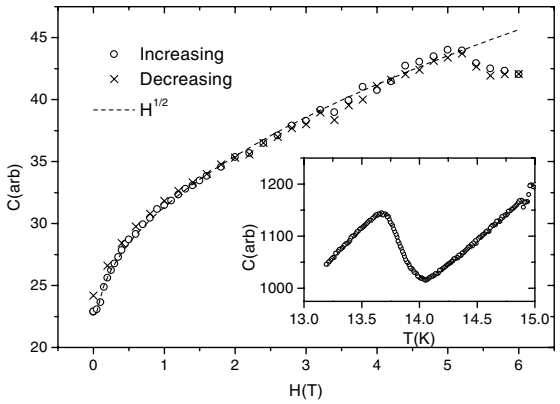

FIG. 1. Field dependence of the specific heat at 2.5 K along the (100) direction. The open circles are with increasing magnetic field, and the crosses are with decreasing field. The dashed line describes $C_0 + b(H - H_0)^{1/2}$, where $C_0 = 23$, $b = 10$, and H_0 is essentially due to the Meissner effect and 0.09 T. Inset: zero-field heat capacity as a function of temperature.

The transverse magnetic field was rotated within the basal plane of YNi_2B_2C by increments of 3° by a computer controlled stepping motor. Repositioning the sample by 33° relative to the thermocouples and apparatus shifts the fourfold pattern, but not the twofold contribution, by that angle. The total heat capacity consists of constant, twofold and fourfold contributions: $C_{\text{total}}(\alpha) = C_0 + C_2(\alpha) + C_4(\alpha)$. The field-independent constant C_0 is due to nonmagnetic contributions, such as the lattice heat capacity and thermally excited nqp's, and is determined experimentally in C vs H data. The twofold contribution $C_2(\alpha)$ comes from our experimental setup and has a functional form of $c_2 \cos 2\alpha$. The Au/Fe thermocouple wire is a major source of this contribution, but misalignment of the basal plane of the sample against the field direction could also lead to the twofold component because of the anisotropy between infield ab-plane and c-axis heat capacities. The dashed line in the upper panel of Fig. 2 is $C_2(\alpha)$; the twofold signal is about 48% of the fourfold component at 1 T and increases with magnetic field up to 55% at 4 T. The circles in the lower panel of Fig. 2 describe the fourfold part $C_4(\alpha)$, which clearly reveals the angular variation.

In the mixed state of an unconventional superconductor, the supercurrent flows around a vortex lead to a Doppler energy shift, $\delta\omega \sim \mathbf{v}_s \cdot \mathbf{k}_F$, where $\mathbf{v}_s$ is the velocity of the superfluid and $\mathbf{k}_F$ is the Fermi momentum of

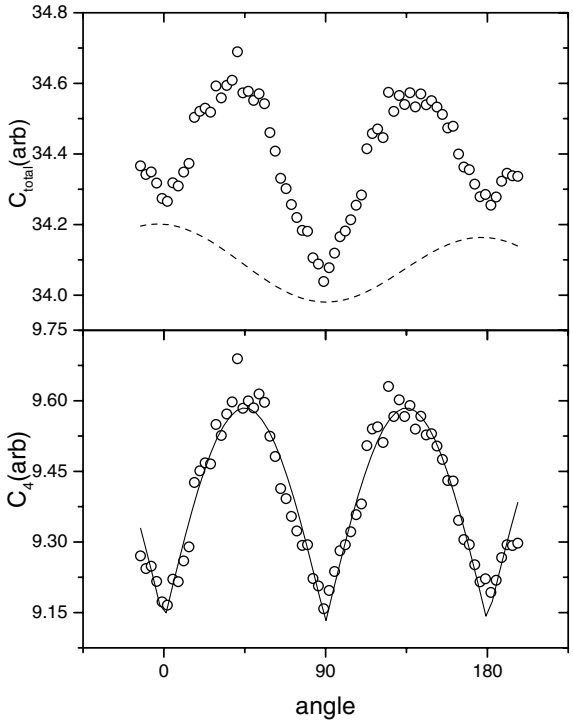

FIG. 2. Field directional dependence of the heat capacity at 2 K in 1 T. The field angle α is measured with respect to the a axis. The top panel shows the total heat capacity (open circles) and the twofold component, $C_2(\alpha)$, relative to the baseline of 34.1 (dashed line). The bottom panel shows the same data after subtracting the background, $C_4(\alpha) = C_{\text{total}}(\alpha) - C_0 - C_2(\alpha)$. The solid line describes a fit with a cusped function, $C_4(\alpha) = c_4(1 + \Gamma|\sin 2\alpha|)$ with $\Gamma = 0.05$.

nodal quasiparticles. When the field direction is normal to the plane containing nodes, the density of states (DOS) is the average over the whole Fermi surface, leading to a square-root field dependence [15]. When the field is in the nodal plane, however, the Doppler shift has a field-direction dependence as well, $\delta\omega \approx \frac{E_h}{\rho}\sin\beta\sin(\phi - \alpha)$ [17]. Here ϕ is an azimuthal angle of the gap node and β is a vortex current winding angle. $E_h = \frac{a\hbar v_F}{2}\sqrt{\pi H/\Phi_0}$ is the energy scale associated with the Doppler effect. The geometrical constant a is order of unity, v_F is the Fermi velocity, and Φ_0 is the flux quantum. The variable $\rho = r/R$, where r is the distance from the vortex core and $2R$ is the intervortex distance. Working in the 2D limit, Vekhter *et al.* calculated the DOS, $N \approx (N_1 + N_2)/2$, for an in-plane magnetic field when $\omega, E_h \ll \Delta_0$ and for four nodes at angles α_n from orthogonal axes in a plane:

$$\frac{N_i(\omega, h, \alpha)}{N_0} = \begin{cases} \frac{\omega}{\Delta_0}\left(1 + \frac{1}{2x^2}\right) & (x = \omega/E_i \geq 1), \\ \frac{E_i}{\pi\Delta_0 x}\left[(1 + 2x^2)\arcsin x + 3x\sqrt{1 - x^2}\right] & (x \leq 1), \end{cases} \tag{1}$$

where $i = 1, 2$, $E_1 = E_h|\sin(\alpha_n - \alpha)|$, and $E_2 = E_h|\cos(\alpha_n - \alpha)|$. N_0 is the normal-state density of states and $h = H/H_{c2}$. The directional dependence of the Doppler effect, therefore, leads to the oscillation of the DOS between minima along nodes and maxima along antinodes. At $T = 0$ K, the oscillation is cusped with a contrast of $1/\sqrt{2}$ between the minima and the maxima and is independent of the magnetic field. At a finite temperature, however, the sharp contrast is washed out and the DOS oscillation now depends on the magnetic field.

As seen in Fig. 2, our data are well described by the cusped function $|\sin 2\alpha|$ which will be used in the analysis of the fourfold variation. To make a quantitative analysis, we fit our data to $C_4(h, \alpha) = c_4(1 + \Gamma|\sin 2\alpha|)$. The coefficient c_4 and the angular contrast Γ were treated as field dependent fitting parameters. The solid line in the lower panel of Fig. 2 shows the fit with $\Gamma = 0.05$ in 1 T. The sharp minima along $\langle 100 \rangle$ indicate that there exist gap minima or nodal structures along those directions, consistent with the angular thermal conductivity measurement [3].

The contrast Γ depends on the gap geometry and dimensionality of the superconductor. The Vekhter *et al.* model above assumes the Fermi momentum of nqp's to be restricted to the nodal plane. Recent band calculations show that YNi_2B_2C has a 3D electronic structure in spite of its layered structure [6]. A more realistic calculation, therefore, is to allow nqp Fermi momentum out of the nodal planes, which decreases the amplitude of the angular variation. Following Won *et al.* [21], we use a modulated cylindrical Fermi surface and account for the 3D effect by replacing the Doppler related energies E_1 and E_2 by $E_1^{3D} = E_h[\sin^2(\alpha_n - \alpha) + \cos^2\theta]^{1/2}$ and $E_2^{3D} = E_h[\cos^2(\alpha_n - \alpha) + \cos^2\theta]^{1/2}$, respectively, and integrate the DOS over polar angle θ:

$$N(w, h, \alpha) = \frac{1}{2\pi}\int_0^{2\pi}\frac{1}{2}[N_1(w, h, \alpha, \theta) + N_2(w, h, \alpha, \theta)]d\theta. \quad (2)$$

The heat capacity ratio, $C(2K, h, \alpha)/C(2K, h, 0)$, calculated from the DOS, is displayed as a 3D surface vs magnetic field angle α (x axis) and H (y axis) in Fig. 3(a). In Fig. 3(b), we show the experimentally obtained data sets after subtraction of the background contributions. Since the in-plane oscillation is due only to the Doppler effect, $C_4(2K, h, \alpha)/C_4(2K, h, 0)$ corresponds to the theory. We used 0.6, 1, 1.5, and 2 T data sets to construct the contour both in numerical and experimental plots. The Doppler energy scale E_h was adjusted to get a best fit, giving the Fermi velocity of $v_F = \sqrt{v_a v_c} = 1.3 \times 10^7$ cm/s which is comparable to other reported values [22]. We used the geometrical constant $a = 1$ and $\Delta = 1.76 k_B T_c$. Note that the angle contrast between experiment and theory are in good agreement suggesting that we are directly observing Doppler-shift generated nqp's. The periodicity of the peaks is $\pi/2$ and the oscillations grow with increasing field because of the increased Doppler energy.

Figure 4 compares the contrast between node and antinode, $\Gamma(2K, h) = [C(2K, h, \pi/4) - C(2K, h, 0)]/C(2K, h, 0)$, from experiment (open circles) with numerical values (dashed line). Above $h = 0.5$, the data deviate from the theoretical prediction. One source of deviation is the Zeeman energy splitting μH, where μ is Bohr magneton, discussed recently by Whelan and Carbotte [23]. At a critical field H_c, Zeeman and Doppler energy scales

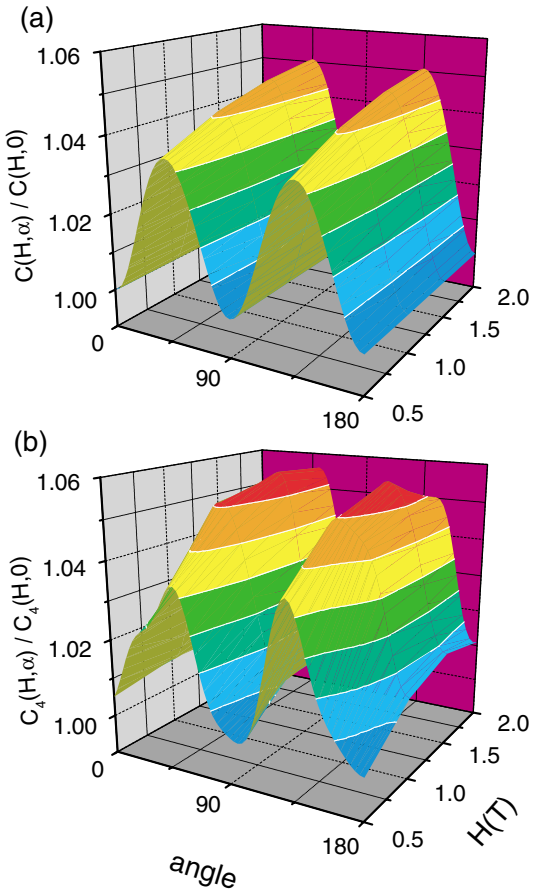

FIG. 3 (color). The 3D surface plots describe magnetic field-angle (x-axis) and field-intensity (y-axis) dependence of the in-plane specific heat ratio at 2 K: $C(h, \alpha)/C(h, 0)$. Plot (a) is a numerical calculation of the specific heat due to nodal quasiparticles in a 3D system, and plot (b) is experimental data taken at 2 K in the vortex phase. The experimental data were FFT low-pass filtered with a cutoff frequency of 0.03 Hz with angles being considered as time. Both plots (a) and (b) were constructed with 0.6, 1, 1.5, and 2 T data sets.

become comparable and the DOS variation with field angle vanishes. It is unlikely, however, that the deviation comes from the effect because the critical field is $\sim 10^2$ T. A more likely possibility is that the deviation is evidence that the core-state contribution to the electronic specific heat becomes significant in the high field regime. When we include the core states, the parameter C_4 consists of the core and the nodal contributions: $C_4(\alpha) = C_{\text{core}} + C_{\text{node}}(\alpha)$. Since the oscillation anisotropy Γ measures the amplitude of the fourfold pattern against the nodal part only, we need to subtract the core part from the C_4, resulting in an increased anisotropy in our data. In order for a quantitative analysis, it is essential to distinguish the contributions from the core states and the extended states.

The inset of the Fig. 4 shows the contrast Γ vs temperature in 1 T. The basal plane of the sample was misaligned by 26° from the field direction, which produced a larger twofold contribution as was expected due to the

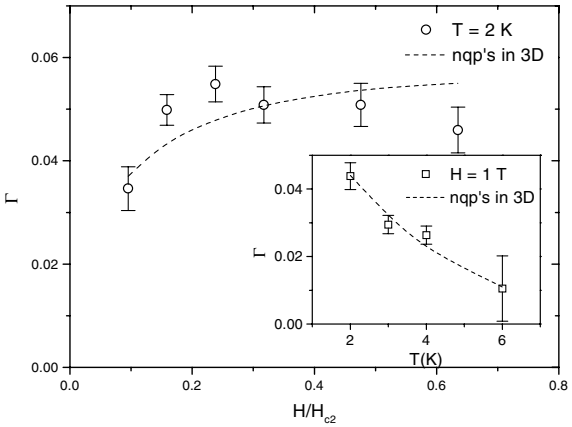

FIG. 4. The oscillation amplitude Γ is shown against the reduced field, H/H_{c2}, at 2 K where H_{c2} is 6.3 T. The dashed lines in the main graph and in the inset are numerical estimations of the angular contrast by nqp's in 3D with the Fermi velocity $v_F = 1.3 \times 10^7$ cm/sec. Inset: the oscillation amplitude was shown against temperature in 1 T.

heat capacity anisotropy between the *ab* plane and the *c* axis. The temperature dependence of the anisotropy was compared with the 3D nqp model that was used in the above analysis. The dashed line is the estimated anisotropy with the same Doppler energy scale with $v_F = 1.3 \times 10^7$ cm/sec. It explains the temperature dependence of the oscillation amplitude very well, corroborating that the nodal quasiparticles are Doppler shifted.

Before concluding this Letter, we discuss the possible pairing symmetries of YNi_2B_2C. Observation of the fourfold angular variation in our heat capacity measurement limits the candidates to those with gap minima or nodes with singlet pairing states such as anisotropic *s* wave, *d* wave, or mixtures of two or more order parameters. Recently, Izawa *et al.* reported a clear fourfold pattern in the *c*-axis thermal conductivity at 0.27 K, which sets the gap-anisotropy ratio to be much higher than 100 [3]. One can still argue for gap minima, but a more natural explanation will be the presence of nodes in momentum space. We note that the field-angle heat capacity will have a fourfold pattern for both *d*-wave and anisotropic *s*-wave gaps with nodes.

In summary, we have reported the first direct evidence for a variation of the density of states of nodal quasiparticles due to a field-induced Doppler energy shift through a fourfold field-angle oscillation in the heat capacity. The angular variation, together with the $\sqrt{H}$ variation of the heat capacity at 2.5 K, strongly suggests that the gap function is extremely anisotropic or, more likely, that YNi_2B_2C is an unconventional superconductor. The magnetic field-angle, field-intensity, and temperature dependences of the heat capacity are in quantitative agreement with a model in which the fourfold pattern arises from Doppler-enhanced, fully 3D nodal quasiparticles with momenta in $\langle 100 \rangle$ directions.

This project was supported in part by NSF Grant No. DMR 99-72087 and at Pohang by the Ministry of Science and Technology of Korea through the Creative Research Initiative Program. X-ray measurements were carried out in the Center for Microanalysis of Materials, University of Illinois, which is partially supported by the U.S. Department of Energy under Grant No. DEFG02-91-ER45439. We thank H. Yanagihara and C. D. Benson for help in building the probe. T. P. thanks N. Goldenfeld for stimulating comments and discussions.

[1] F. Yu, M. B. Salamon, and A. J. Leggett, Phys. Rev. Lett. **74**, 5136 (1995).
[2] H. Aubin, K. Behnia, and M. Ribault, Phys. Rev. Lett. **78**, 2624 (1997).
[3] K. Izawa, K. Kamata, Y. Nakajima, Y. Matsuda, and T. Watanabe, Phys. Rev. Lett. **89**, 137006 (2002).
[4] Y. Wang, B. Revaz, A. Erb, and A. Junod, Phys. Rev. B **63**, 094508 (2001).
[5] S. A. Carter *et al.*, Phys. Rev. B **50**, 4216 (1994).
[6] L. F. Mattheis, Phys. Rev. B **49**, 13 279 (1994).
[7] H. Michor, T. Holubar, C. Dusek, and G. Hilscher, Phys. Rev. B **52**, 16 165 (1995).
[8] R. S. Gonnelli, A. Morello, G. A. Ummarino, V. A. Stepanov, G. Behr, G. Graw, S. V. Shulga, and S. L. Drechsler, Int. J. Mod. Phys. B **14**, 2840 (2000).
[9] S. Manalo and E. Schachinger, J. Low Temp. Phys. **123**, 149 (2001).
[10] M. Nohara, M. Isshiki, H. Takagi, and R. J. Cava, J. Phys. Soc. Jpn. **66**, 1888 (1997).
[11] E. Boaknin, R.W. Hill, C. Proust, C. Lupien, and L. Taillefer, Phys. Rev. Lett. **87**, 237001 (2001).
[12] I.-S. Yang, M.V. Klein, S. L. Cooper, P. C. Canfield, B. K. Cho, and S.-I. Lee, Phys. Rev. B **62**, 1291 (2000).
[13] K. Izawa, A. Shibata, Y. Matsuda, Y. Kato, H. Takeya, K. Hirata, C. J. van der Beek, and M. Konczykowski, Phys. Rev. Lett. **86**, 1327 (2001).
[14] K. Maki, P. Thalmeier, and H. Won, Phys. Rev. B **65**, 140502 (2002).
[15] G. E. Volovik, JETP Lett. **58**, 469 (1993).
[16] V. Metlushko, U. Welp, A. Koshelev, I. Aranson, G.W. Crabtree, and P. C. Canfield, Phys. Rev. Lett. **79**, 1738 (1997).
[17] I. Vekhter, P. J. Hirschfeld, J. P. Carbotte, and E. J. Nicol, Phys. Rev. B **59**, R9023 (1999).
[18] B. K. Cho, P. C. Canfield, L. L. Miller, D. C. Johnston, W. P. Beyermann, and A. Yatskar, Phys. Rev. B **52**, 3684 (1995).
[19] T. Park, M. B. Salamon, C. U. Jung, M.-S. Park, K. Kim, and S.-I. Lee, Phys. Rev. B **66**, 134515 (2002).
[20] M. Ichioka, A. Hasegawa, and K. Machida, Phys. Rev. B **59**, 184 (1999).
[21] H. Won and K. Maki, Europhys. Lett. **56**, 729 (2001).
[22] V. G. Kogan, M. Bullock, B. Harmon, P. Miranovic, Lj. Dobrosavljevic-Grujic, P. L. Gammel, and D. J. Bishop, Phys. Rev. B **55**, R8693 (1997).
[23] N. D. Whelan and J. P. Carbotte, Phys. Rev. B **62**, 14 511 (2000).